Cement and Concrete Research 42 (2012) 124–133

Contents lists available at SciVerse ScienceDirect

Cement and Concrete Research

journal homepage: http://ees.elsevier.com/CEMCON/default.asp

Effect of the addition of red mud on the corrosion parameters of reinforced concrete ☆

D.V. Ribeiro [a,*], J.A. Labrincha [b], M.R. Morelli [c]

[a] Department of Materials Science and Technology, Federal University of Bahia, Rua Aristides Novis, 02. Federação. 40210-630. Salvador/BA, Brazil
[b] Ceramics and Glass Engineering Dept., University of Aveiro & CICECO, Campus Universitário de Santiago, 3810-193. Aveiro, Portugal
[c] Department of Materials Engineering, Federal University of São Carlos, Rodovia Washington Luis, Km 235. 13566-550. São Carlos/SP, Brazil

ARTICLE INFO

Article history:
Received 16 November 2010
Accepted 13 September 2011

Keywords:
Concrete (E)
Red mud
Diffusion (C)
Corrosion (C)
Electrochemical properties (C)

ABSTRACT

Red mud, the main waste generated in aluminum and alumina production by the Bayer process, is considered "hazardous" due to its high pH. The characteristic of high alkalinity associated with the presence of aluminosilicates facilitates the assimilation and formation of compounds by reaction with chloride ions. The high pH also provides greater protection of rebars, which is reflected in the low corrosion potential and high electrical resistivity (filler effect) of concrete. In this study, the chloride concentration was monitored by measuring the conductivity of the anolyte. Red mud proved to be a promising additive for concrete to inhibit the corrosion process. The corrosion potential was monitored by electrochemical measurements and the electrical resistivity was evaluated using sensors embedded in concrete test specimens. The results showed that the addition of red mud is beneficial to concrete, reducing its chloride migration rate (diffusion coefficients) and corrosion potential and increasing its electrical resistivity.

1. Introduction

The world's production of bauxite in 2008 was 205 million tons, and the main producing countries were Australia, China, Brazil, Guinea, India and Jamaica. Ranking third in worldwide production in 2008, Brazil produced 26.6 million tons of bauxite. It also has the world's third largest bauxite ore reserves (around 3.5 billion tons), concentrated mainly in the northern part of the country (state of Pará) [1]. Roughly 0.3–1.0 tons of red mud waste are generated per ton of aluminum produced. Brazil has discarded about 10.6 million tons/year of caustic red mud in recent years and the worldwide generation of red mud exceeds 117 million tons/year [2].

The storage of large quantities of alkaline residue (red mud) is expensive (between 1 and 2% of the price of alumina), requiring large disposal areas (about 1 km^2 for five years of production for a factory producing 1 million tons of alumina per year) and causing serious environmental problems [3]. Therefore, the use of this waste in cement matrices is very attractive since the high amount of cement consumed worldwide is compatible with the high generation of this waste.

Alkaline matrices such as those provided by Portland cement in mortars and concrete are commonly used in waste conditioning. They are inexpensive, have an extensively documented history of safe use, and are a draw-upon readily-accessible technology. Alkalinity greatly reduces the solubility of many hazardous inorganic species and inhibits microbiological processes. Moreover, since these matrices require water for hydration, they may readily incorporate wet wastes [1] such as red mud.

The search for an economically and environmentally viable alternative has led to the study of red mud for various applications, such as alternative construction material [3], an adsorbent for the removal of heavy metals from aqueous solutions [4], building materials, namely bricks [5,6], ceramics and tiles [7], ceramic glazes [8], red mud–polymer composite panels as wood substitutes [9], and iron-rich cement [10,11].

The high alkalinity of red mud, which was initially a factor of environmental concern, has proved to be the main advantage of using red mud as a rebar corrosion inhibitor in reinforced concrete without affecting its passivity. To ascertain its possible use, rebar corrosiveness was evaluated by monitoring chloride diffusion, corrosion potential and electrical resistivity.

1.1. Chloride migration test

It is widely accepted that the presence of chloride ions in concrete structures is responsible for the breakdown of the passive film and subsequent corrosion of steel bars. Several investigations [12–14] have used the accelerated migration test to assess the resistance of concrete to the penetration of chloride ions. Initially, these tests were employed to evaluate the penetration of chloride ions by evaluating the total load passing through, according to the ASTM C 1202/1992 standard, and the steady-state diffusion coefficients of chloride ions, as proposed by Andrade [15].

More recently, several authors have used migration tests to calculate the diffusion coefficient also in the nonsteady state [12,13].

☆ This project was not funded by Alcoa Brazil.
* Corresponding author. Tel.: +55 71 32839852; fax: +55 16 33615404.
E-mail address: verasribeiro@hotmail.com (D.V. Ribeiro).

0008-8846/$ – see front matter © 2011 Elsevier Ltd. All rights reserved.
doi:10.1016/j.cemconres.2011.09.002

However, no satisfactory correlation has been found among theoretical results obtained by several different techniques, although all the tests are based on the induction of ions in response to an external electric field [15].

1.2. Corrosion potential

Monitoring of the corrosion potential enables changes in the electrochemical corrosion process to be recorded, which can be quite interesting in monitoring structures. However, the results indicate a balance between anodic and cathodic reactions, without providing quantitative information, i.e., information about the reinforcement corrosion rate cannot be obtained. Thus, the rebar corrosion potential provides a rough indication of a rebar corrosion situation or a rebar passive state.

The ASTM C-876/91 standard presents a correlation between corrosion potential ranges and the probability of corrosion occurrence as a criterion for corrosion evaluation, taking as reference a copper/copper sulfate electrode ($Cu/CuSO_4$, Cu^{2+}). This and other correlations are presented in Table 1.

1.3. Electrical resistivity

Electrical resistivity is an important property of concrete and indicates its ability to resist the passage of electrical current. This property is fundamentally related to fluid permeability and ion diffusivity through the pores and, in the case of concrete, is closely related to the corrosion rate of steel reinforcement bars [14].

The presence of salts such as chlorides, sulfates and nitrates enables reinforcement bar corrosion because salts are strong electrolytes (low resistivity), allowing for the flow of electrons and corrosion of the reinforcement. Resistivity values indicate the probability of reinforcement corrosion but these values are not fully recognized internationally and vary according to the methodology employed. Commonly used reference values (Table 2) are found in the CEB standard 192 or the European CE Bulletin – COST 509 (corrosion and protection of metals in contact with concrete) presented by Polder [16].

Among the factors that influence the resistivity of concrete, Santos [14] cites: the characteristics of the concrete (water/cement ratio, type and amount of aggregates, cement consumption, the presence of chemical additives and additions, degree of hydration); environmental characteristics (temperature and relative humidity) and the action of aggressive agents (chloride penetration and carbonation).

2. Materials and methods

2.1. Materials

The concrete was produced with a Brazilian Portland cement (CPII Z-32, to the Brazilian NBR 11578 standard), which is equivalent to the ASTM C 596 standard (*Pozzolan-modified Portland cement*). This cement contains pozzolan and is one of the cements most widely used in the state of São Paulo, Brazil. The coarse aggregate was dense, crushed granite stone and the fine aggregate was natural siliceous sand commercially available in São Carlos, SP, Brazil.

Table 2
Resistivity values and risk of corrosion of reinforcement bars, according to the CEB-192 standard and the European CE Bulletin – COST 509 *apud* Polder [16].

Concrete resistivity (KΩ.cm)		Risk of corrosion
CEB-192	COST 509	
>20	>100	Negligible
10–20	50–100	Low
–	10–50	Moderate
5–10	<10	High
<5	–	Very high

The red mud was supplied by ALCOA Brazil and came from Poços de Caldas, MG. It is a mixture containing about 60% of solids, collected immediately after alumina recovery from the digestion process (Bayer process).

2.2. Methods

2.2.1. Characterization of materials and preparation of concrete samples

Characterization of the materials involved X-ray diffraction (Rigaku Geigerflex ME 210GF2 diffractometer) and X-ray fluorescence (Philips PW1480 X-ray fluorescence spectrometer) analyses. Physical parameters such as the specific surface area (estimated by BET, using a Micromeritics Gemini 2370V1.02 surface area analyzer) and specific gravity (Micromeritics Accupyc 1330V2.01 helium pycnometer) were also determined.

The concrete mix proportions were 1.0 (Portland cement): 1.5 (fine aggregate): 1.3 (coarse aggregate) and the water/cement ratio was 0.5. The mortar content was 75% and the cement consumption was 526 kg/m^3. After mixing, a vibrating table was used to ensure efficient compaction. Concretes containing distinct additions of red mud (10, 20, and 30% in weight) were prepared and analyzed.

The specimens for the migration tests were cylindrical (50 mm in diameter and 100 mm in length). These specimens were cut into 40 mm thick slices, and the end portions of each cylinder were discarded to minimize heterogeneities and ensure water saturation. The corrosion potential was measured using prismatic specimens ($50\times70\times90$ mm^3) into which steel bars were inserted during molding. The electrical resistivity of the concrete was tested using molded concrete blocks ($200\times200\times100$ mm^3) with sensors embedded in them.

All the specimens were unmolded 24 h after being cast and were cured for 28 days in a humid chamber (>95% HR). A minimum of 4 samples were tested in all determinations.

2.2.2. Chloride migration test

The American ASTM C-1202/97 standard (Standard Test Method for Electrical Indication of Concretes Ability to Resist Chloride Ion

Table 1
Probability of rebar corrosion activity as a function of ranges of corrosion potential of various reference electrodes in accordance with the ASTM C-876/91 standard.

Electrode	Probability of rebar corrosion activity		
	<10%	10%–90%	>90%
NHE[a]	>0.118 V	(0.118 V) − (0.032 V)	<−0.032 V
$Cu/CuSO_4$,Cu^{2+} (ASTM C 876)	>−0.200 V	(−0.200 V) − (0.350 V)	<−0.350 V
Hg,Hg_2Cl_2/KCl (saturated solution)[b]	>−0.124 V	(−0.124 V) − (0.274 V)	<−0.274 V
Ag,AgCl/KCl (1 M)	>−0.104 V	(−0.104 V) − (0.254 V)	<−0.254 V

[a] Normal Hydrogen Electrode (NHE) standard.
[b] Saturated Calomel Electrode (SCE) used in this work.

Penetration) advocates the use of vacuum saturated samples before submission to migration tests. This procedure has been adopted by other researchers [12,14] to ensure that the penetration of chlorides into the sample was caused predominantly by diffusion. In this work, vacuum saturation was not used; instead, the samples were soaked in water for 24 h prior to testing.

PVC cells were used, consisting of a 50 mm diameter "T" tube with a top cover for output measurements and a side containing the electrode, properly sealed to prevent loss of solution. The specimens were placed at the interface between the two chambers, and were also glued with a silicone-based adhesive. Thus, the ion exchange between cells took place only through the body surface-to-test exposed area. The test setup and its implementation are illustrated in Figs. 1A and B, respectively. A 12-Volt current was applied to the system by means of electrodes positioned at the ends of the cell, which were connected to copper wires from a controlled voltage source.

The principle of the migration test is to apply a potential difference between two cells: the first containing a chloride solution (catholyte chamber) and the other without chlorides (anolyte chamber). The concrete sample is placed between these chambers (Fig. 1) and the external electric potential applied forces the chloride ions to pass through the concrete sample from the first to the second chamber [14]. The positive cell (anolyte chamber) is filled with distilled water to prevent corrosion-induced chloride deposition. A 1 M NaCl solution was used in the negative cell (catholyte chamber).

The concentration of chlorides in the anolyte chamber (initially free of chlorides) was analyzed at regular intervals during the experiment using a portable digital conductivity meter (CD-880, *Instrutemp*). The chloride concentration was estimated based on the correlation between this parameter and the electrical conductivity, as indicated in Fig. 2. Conductivity values were referenced to a temperature of 25 °C, by considering an increase of 2% in the conductivity of the solution when the temperature rose by one degree centigrade.

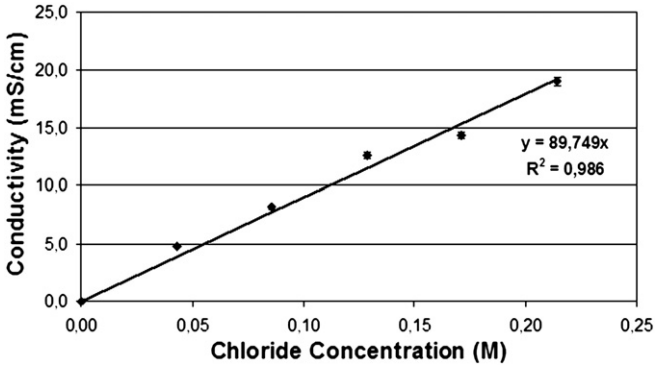

Fig. 2. Experimental relationship between conductivity (at 25 °C) and chloride concentration in the anolyte compartment, which initially contains distilled water.

2.2.3. Corrosion potential

The reinforcement steel bars were weighed on an analytical balance with an accuracy of 0.01 g. The area exposed to chloride attack (about 15.83 cm²) was then delimited by electrical insulating tape, as shown in Fig. 3. The bars were positioned so that the exposed area was located in the central region of the specimens, as illustrated in Fig. 3D.

The corrosion potential is basically verified from a chloride-activated accelerated corrosion test. The electrochemical cell used for corrosion potential measurements was composed of a working electrode, the reinforcement steel bars and the saturated calomel electrode (SCE) used as reference electrode.

Before taking the measurements, the side of the specimens to be measured was pre-moistened with a wet sponge for 1 min. A conductive solution containing 5 mL of neutral detergent to 1 L of water,

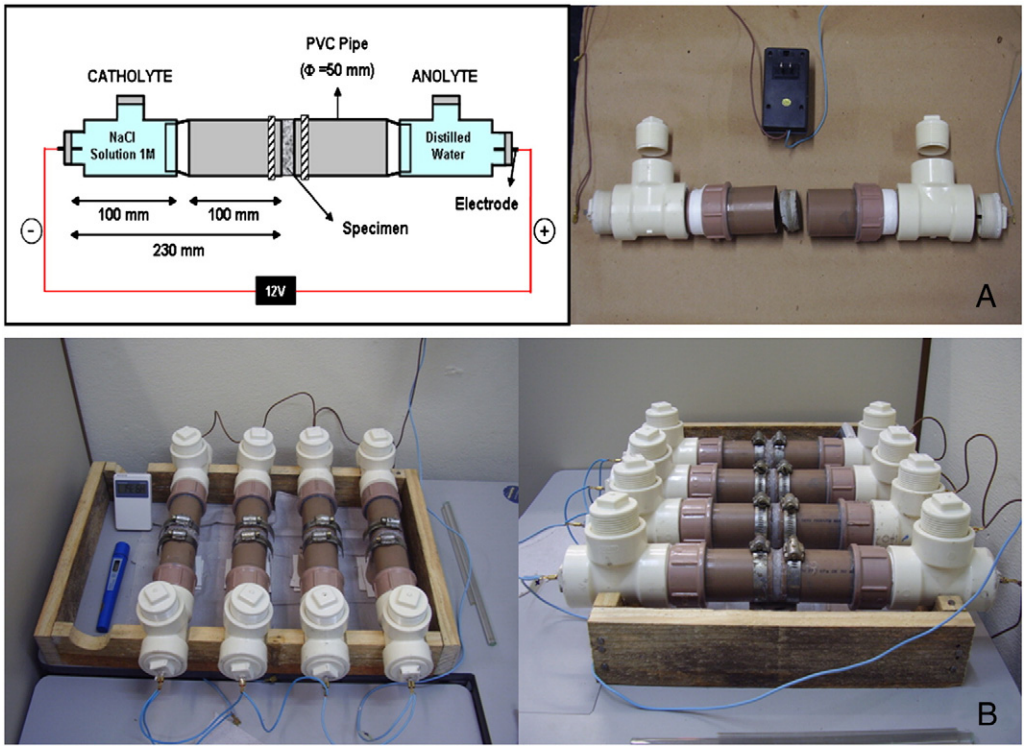

Fig. 1. (A) Setup and assembly of the chloride migration test; (B) chloride migration test apparatus.

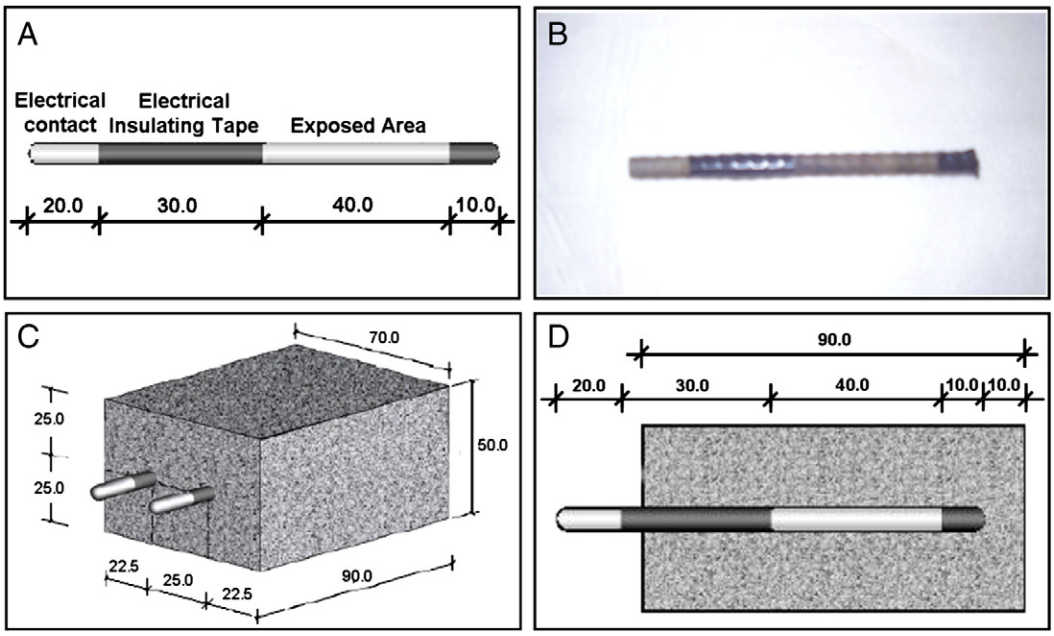

Fig. 3. (A) and (B): Scheme of the exposed area of the rebar delimited (in mm), and (C) and (D): sample dimensions (in mm) and steel rebar positions in concrete samples.

according to the ASTM C-876/91 standard (Standard Test Method for Half-Cell Potentials of Uncoated Reinforcing Steel in Concrete) and an electrical conductivity of 0.15 ± 0.02 mS/cm were used. For the measurements, the reference electrode was positioned approximately at mid-span over the rebar under analysis. The contact between the reference electrode and the specimen was aided with a damp sponge.

The corrosion test was started after 63 days, when the specimens showed a constant mass (1.0 g of variation in two consecutive 24-hour readings) and when the measured corrosion potential indicated the formation of a passive film on the surface of the steel bars ($E_{cor} > -0.124$ V). This reference value corresponds to a lower than 10% possibility of corrosion occurrence, according to the ASTM C 876/91 standard (for the saturated calomel electrode used in this work).

In other works [14,17], it was necessary to define a specific age, or reference age, from which the procedures of the accelerated corrosion tests started. The authors of those studies associated the reference age to the stabilization of the cement hydration process and defined the ages of 63 days [17] and 80 days [14] as sufficient for the cement paste to acquire a relatively well developed physical structure and a significantly high degree of hydration.

After reaching the "safe potential," the specimens were subjected to semi-cycles of partial immersion in 3 wt.% NaCl solution for two days and semi-cycles of drying in a ventilated oven at 50 °C for five days. During the semi-cycle of partial immersion, the level of immersion solution was kept at half height of the specimens. In this condition, the chloride inflow occurs primarily by capillary absorption, since the specimens are first dried, and after the pores become saturated, the inflow occurs by diffusion, which is accelerated due to water evaporation through the exposed concrete. The corrosion potential (E_{corr}) was measured at the end of each semi-cycle.

The active state of corrosion ($E_{corr} < -0.274$ V) or passive state ($E_{corr} > -0.124$ V) was analyzed based on the corrosion potential (E_{corr}), using the saturated calomel electrode (SCE) as reference. The test was concluded when two consecutive and full cycles resulted in corrosion potential values below the critical value ($E_{corr} < -0.274$ V).

After concluding the test, the rebars were extracted from the samples, cleaned according to the ASTM G-1/03 standard, and weighed to determine weight loss and to compare them with the initial value. Thus, the corrosion rate (CR) can be calculated according to Eq. (1).

$$CR = \frac{K.W}{A.T.D} \quad (1)$$

where K = constant (for CR(μm/year), $K = 8.76 \times 10^7$; for CR(g/m^2.year), $K = 8.76 \times 10^7$.D); W = weight loss (grams); A = exposed rebar area (cm^2); T = exposure time (hours); D = steel rebar density (for CA-50

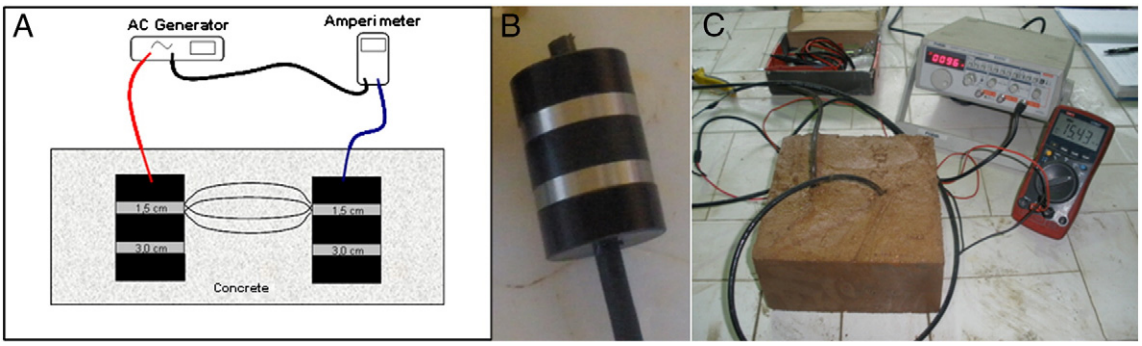

Fig. 4. (A) Schematic diagram of the measurement of concrete electrical resistance, (B) electrical probe used, and (C) electrical current measure.

steel, D = 7.85 g/cm^3). In this study, A = 15.83 cm^2 and T = 4320 h (180 days).

2.2.4. Electrical resistivity

The electrical resistivity of concrete was calculated from the electrical current (I) passing through the specimens. The system, which is shown schematically in Fig. 4, consists of two cylindrical probes, each with two electrodes (different measurement levels) made of stainless steel (rings/washers) and spaced at different layer depths. The probes used in this study were supplied by the Institute of Corrosion (ICorr), which specializes in corrosion studies. The two probes of the system should be placed 10 cm apart.

Through this monitoring system, the ionic resistivity of concrete at each depth can be determined by the paired-electrode technique. An alternating current is applied between the electrodes and the resistivity is determined by measuring the resistance (ΔE/ΔI, Ohm's law) and by a parameter that depends on the geometry of the electrodes and on the distance between them (A/L). Thus, the resistivity (ρ) is calculated according to Eq. (2):

$$\rho = \frac{V \cdot A}{I \cdot L} \tag{2}$$

For circular electrodes, Eq. (2) is equivalent to:

$$\rho = \frac{2\pi \cdot V \cdot L}{I} \tag{3}$$

where ρ is the electrical resistivity of concrete (Ω.cm); V is the applied voltage; I is the current intensity; A is the area of the side of the specimen in contact with the electrode (cm^2); and L is the distance between the electrodes (cm). The European CE Bulletin – COST 509 (Corrosion and Protection of Metals in Contact with Concrete) was used as the evaluation parameter since it is more stringent in relation to values than those suggested by the CEB-192 standard.

3. Results and discussion

3.1. Materials characterization

The Portland cement used here has a specific surface area of 0.93 m^2/g and a specific gravity of 3.11 kg/dm^3. The sand has a specific surface area of 0.68 m^2/g and a specific gravity of 2.70 kg/dm^3, and is classified as fine sand by the Brazilian NBR 7211 standard. The gravel has a specific gravity of 2.74 kg/dm^3 and a maximum dimension of 19 mm.

The red mud was received as a paste containing about 40% of free water. In this study, the material was dried, crushed, and used as a powder additive. Ideally, if its potential as a constituent of concrete is demonstrated, red mud incorporation should be tested in the as-received condition, thus accounting for the free water present in the mud as a mortar mix component.

Table 3
Chemical composition of red mud estimated by XRF.

Component	Al_2O_3	Fe_2O_3	Na_2O	CaO	SiO_2	K_2O	MnO	TiO_2	Others	LOI[a]
Content (wt.%)	19.87	19.85	7.35	4.61	14.34	1.87	0.21	2.66	1.01	27.20

[a] LOI = loss on ignition.

The specific surface area of bauxite waste is 20.27 m^2/g, according to the particle fineness shown in Fig. 5. Maximum particle size is under 40 μm and the mean value is only about 8 μm. The specific gravity is 2.90 kg/dm^3 and the pH is very high (12.95), exceeding the limit (12.5) for non-hazardous wastes defined by the Brazilian NBR 10004 standard.

Table 3 presents the chemical composition of the waste while Fig. 6 shows the corresponding XRD pattern. As expected, the major components are aluminum hydroxide ($Al(OH)_3$), calcium carbonate ($CaCO_3$), and iron oxide (Fe_2O_3), but the relative amounts of SiO_2, muscovite and FeO(OH) are also relevant. Some of these oxides are also detected by XRD, in addition to aluminum hydroxide and a complex $Na_5Al_3CSi_3O_{15}$ phase.

In the hydration of high-iron Portland cement, the calcium aluminate ferrite phase reacts with calcium sulfate, yielding the ettringite phase. The formation of ettringite in high-iron cements progresses more slowly than in cements with Fe_2O_3 contents corresponding to ordinary or low-iron Portland cements [29].

The high fineness (20.27 m^2/g of surface area) of red mud can interfere with drying shrinkage because, due to its fineness, it retains a reasonable amount of water.

A high iron oxide content in concrete structures can promote the formation of hydrated iron oxide (Fe_2O_3 nH_2O), which, to occupy its space, exerts a pressure in the order of 15 MPa on its confining material, which suffices to fracture the concrete [29]. However, this phenomenon was not observed in the specimens used in this study.

Manso et al. [30] examined the effect of adding a waste with high iron oxide content (EAF slag) on the durability of concrete. These authors found that, after freezing and thawing cycles, the internal pressure of ice in the accessible pores of the concrete (matrix and aggregates), allied to thermal changes, caused surface spalling of the samples and drastically reduced their compressive strength. A similar behavior was observed after wetting and drying tests. In this case, damage was produced by the combination of two effects: thermal dilation and contraction, and shrinkage due to variations in humidity [30].

On the other hand, Pellegrino and Gaddo [31] obtained excellent results and their specimens showed no significant surface deterioration despite the severity of the tests. Thus, it is clear that the

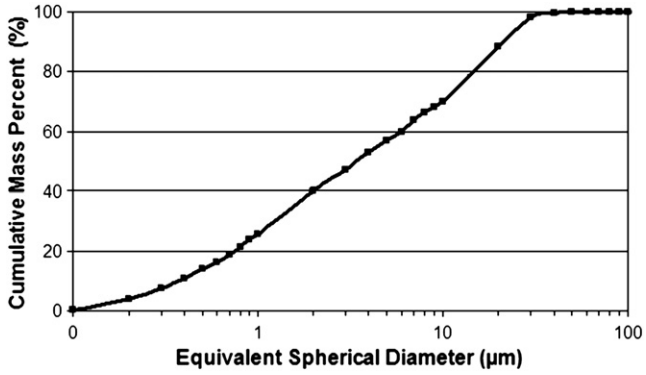

Fig. 5. Particle size distribution of the dry red mud.

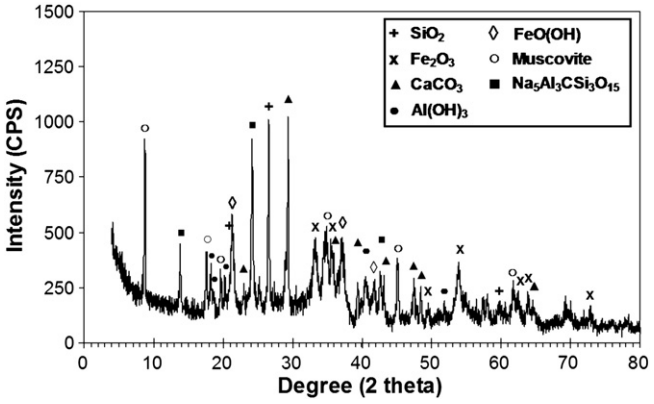

Fig. 6. X-ray diffraction (XRD) pattern of dry red mud.

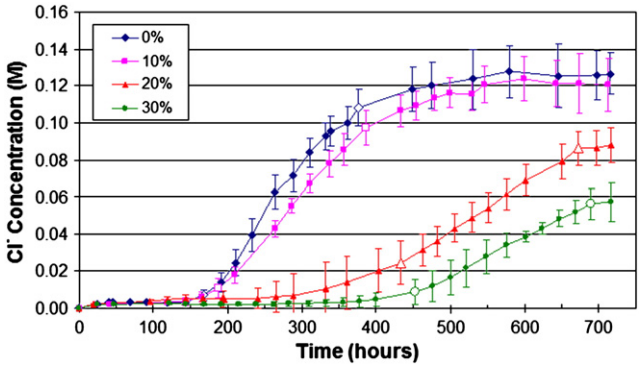

Fig. 7. Evolution of Cl^- concentration in the anolyte chamber of a migration test cell over time, in concrete samples containing distinct amounts of red mud waste (0–30%).

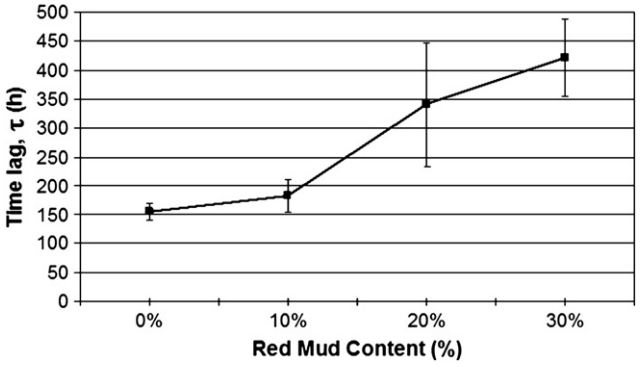

Fig. 9. Time lag estimated from chloride migration tests as a function of red mud content added to concrete cured for 28 days.

implications of high iron oxide content for concrete durability are not yet well understood.

The high loss on ignition (LOI) observed in red mud (27.2%) may lead to consequences in the long-term durability of concrete. Due to the presence of hydrated compounds and residual organic matter, a highly porous cement matrix may be observed, which reflects the low stability of the concrete in terms of wetting–drying and freeze–thaw cycles.

3.2. Chloride migration test

Fig. 7 shows the evolution of chloride concentration in the anolyte chamber during migration tests. As expected, the Cl^- concentration increases over time once the voltage is applied, following the predictable trend.

Initially, there is a period in which the amount of chlorides passing into the anolyte chamber is negligible. Its duration corresponds to the so-called "time lag" (τ), and can be defined as the time required for chlorides to pass through the concrete disc, causing its saturation. This period of time will later serve as the basis for estimating the D_{ns} values. After this period, the flux of chloride ions through the specimen becomes constant, which corresponds to the steady-state period.

The time lag is determined empirically from the intersection between the extension of the line that characterizes the steady-state and the time axis, according to the diagram in Fig. 8.

Fig. 9 shows that the time lag increases with increasing waste content, probably due to the reduction of a relative number of capillary pores [18]. Moreover, the mud particles may close or interrupt the connectivity between some of those pores, thus diminishing the capillary suction of the concrete and hindering the transport of substances [19]. This occurs even in samples showing higher total porosity, meaning that within certain limits this parameter is not relevant. Microstructural changes should therefore be accounted for to better explain behavioral differences between the samples.

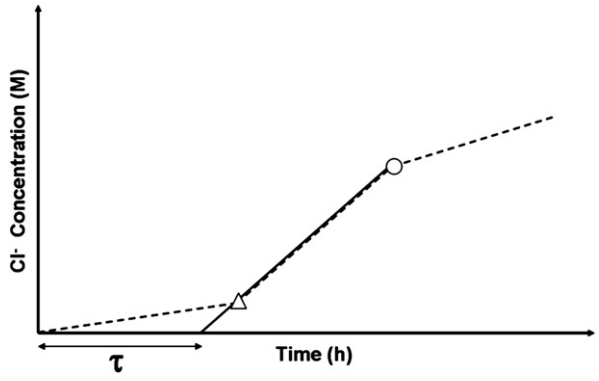

Fig. 8. Experimental determination of the time lag (τ); start (Δ) and end ($\circ$) of the steady-state diffusion stage, whose diffusion coefficient is D_s.

After the time lag, the flux of chloride ions through the specimen increases at a constant rate, which corresponds to the steady-state regime [12]. The *steady-state* diffusion coefficient (D_s) in migration tests is estimated using the Modified Nernst–Planck equation:

$$D_S = \frac{J_{Cl} RTl}{zFC_{Cl}\gamma\Delta\Phi} \tag{4}$$

where J_{Cl} = flux of chloride ions (mol/cm^2.s); R = gas constant (1.9872 cal/mol.K); T = temperature (K); l = sample thickness (4 cm); z = ion valence (chlorides = 1); F = Faraday's constant (23063 cal/volt.eq); C_{cl} = chloride concentration in the catholyte (mol/cm^3); γ = activity coefficient of the catholyte solution (Cl^- = 0.657) and $\Delta\Phi$ = effective applied voltage (12 V).

The chloride ion flux (J_{Cl}) represents the speed at which the ions are transported through the concrete, and the *steady-state* and *nonsteady-state* diffusion coefficients are calculated based on this flux. These coefficients can be calculated using the linear slope of the graph representing the evolution of the chloride concentration in the anodic cell as a function of time (see Fig. 8):

$$J_{Cl} = \frac{V}{A} \times \frac{dC}{dt} \tag{5}$$

where A = exposed area (cm²) and V = volume of the cathodic chamber (cm^3).

The *steady-state* diffusion coefficient (D_{ns}) was calculated as follows. First, by estimating the enhancement or progress ratio obtained by applying an electrical field, comparing the time that chlorides would require under natural conditions of diffusion to reach the penetration depth observed in migration tests (t_{dif}), according to Eqs. (6) and (7) [12].

$$\frac{1}{t_{dif}} = \frac{6}{\tau\nu^2} \times \left[\nu \times \coth\frac{\nu}{2} - 2\right] \tag{6}$$

$$\nu = \frac{ze\Delta\Phi}{kT} \tag{7}$$

where τ = time lag in the migration test; t_{dif} = time equivalent if no electrical field were applied (s); e = 1.6 10^{-19} C; k = Boltzmann's constant (1.38 10^{-23} J/K).

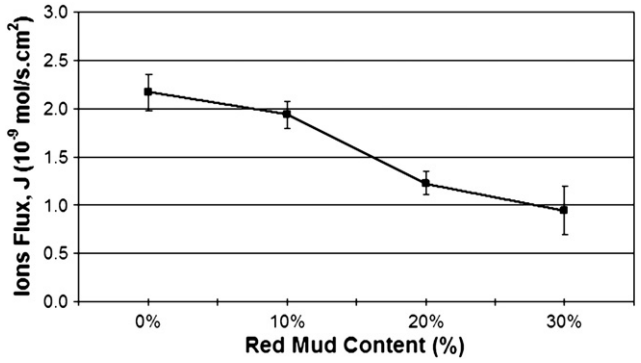

Fig. 10. Flow of chloride ions estimated from the migration tests as a function of red mud content in the concrete cured for 28 days.

This mathematical solution allows migration tests to be "converted" into natural tests. In other words, using this "equivalent" time, t_{dif}, D_{ns} is obtained directly from Eq. (8):

$$D_{ns} = \frac{l^2}{3t_{dif}} \tag{8}$$

where l = specimen thickness (cm).

Fig. 10 shows the flow of chloride ions, J_{Cl}, through the concrete as a function of red mud content in the material. This parameter represents the speed at which the ions are transported through the concrete and from which the *steady-state and nonsteady-state* diffusion coefficients (Fig. 11) are calculated. A clear decrease is observed in samples containing increasing amounts of waste. This is very positive because it reveals a delay in the onset of the corrosion process caused by the migration of chloride ions. These observations are in agreement with findings reported by Santos [16] and Aïtcin [20], who showed the tendency of supplementary cementitious materials (such as red mud) to significantly reduce the mobility of chloride ions, reflecting the effect of increased tortuosity and better pore diameter distribution resulting from the pozzolanic reactions, which hinder ionic movement.

Moreover, red mud contains mineralogical phases such as sodium aluminosilicates, known as sodalites, i.e., zeolite-type compounds with an extremely high ion-exchange capacity, which makes red mud a good absorber of heavy metals [21] and influences their surface properties [22], including the formation of compounds by reaction with chloride ions. Other authors [23] also cite the importance of the presence of aluminates, which play an important role in anchoring the chloride ions, which would otherwise be free and available to start the corrosion process.

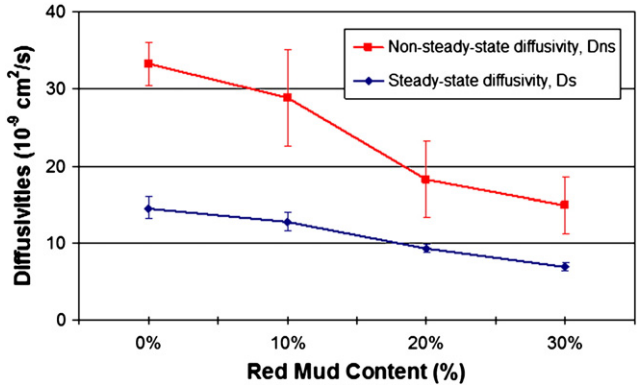

Fig. 11. Steady-state and nonsteady-state diffusion coefficients of chloride ions estimated from migration tests as a function of red mud content in concrete cured for 28 days.

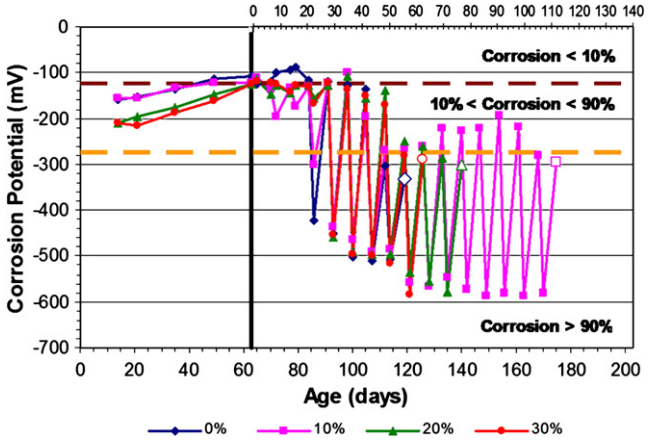

Fig. 12. Evolution of the corrosion potential of rebars embedded in reinforced concrete specimens containing red mud, as a function of age.

The aspects discussed in the above paragraph are also reflected in the steady-state and nonsteady-state diffusion coefficients of chloride ions shown in Fig. 11, both of which decreased due to the addition of a higher red mud content.

3.3. Corrosion potential

Based on the corrosion potential measurements an analysis was made of the onset of rebar corrosion, i.e., the moment when the potential was below −274 mV (the probability of corrosion exceeds 90% for the saturated calomel electrode). Results obtained by Bauer, as described by Santos [14] show that, in most cases, the evaluation of the corrosion onset period based on corrosion potential tests is consistent with assessments based on more accurate electrochemical parameters such as corrosion intensity (i_{corr}).

Fig. 12 presents the results of the corrosion potential measurements. In the first 63 days, the specimens were not subjected to wetting and drying cycles in NaCl solution until the "safe potential" (−124 mV) was reached, and the tests were interrupted when the "unsafe potential" (−274 mV) was reached in two consecutive dry state measurements. The values represent the average of six measurements taken for each composition. The error bars were not placed in graphs because they would render the graphs very confusing and difficult to visualize. However, it can be stated that the results were highly reproducible, with a variation of less than 6%.

One of the aspects of the test procedure adopted is that the rebar corrosion potential varied throughout the test, showing more negative or more positive values depending on the semi-cycle to which the specimen was subjected.

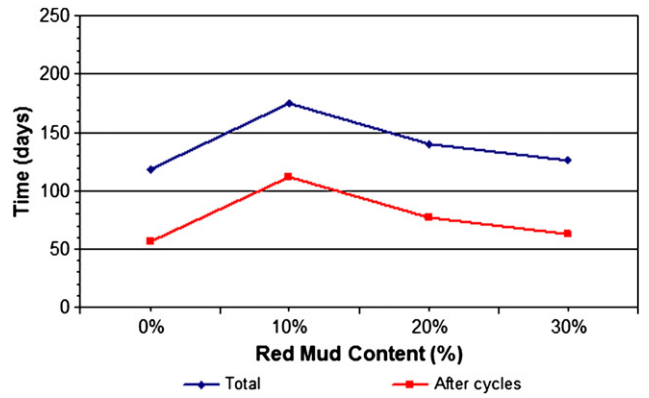

Fig. 13. Rebar corrosion onset period as a function of red mud content.

The most positive corrosion potential values were recorded after the drying cycles because, due to the decreasing amount of electrolyte, the concentration of dissolved substances increased. In fact, according to the Nernst equation, the equilibrium potential increases with the increase in activity, i.e., the increase in the effective concentrations of oxidized substances. Studies by Santos [14] confirm this behavior and show an inverse correlation between the corrosion potential and the concrete's moisture content, indicating that an increase in moisture content implies a decrease in the measured rebar corrosion potential.

According to the results shown in Fig. 12, the reference samples showed a greater difference between the corrosion potential measurements in the wet and dry states (0%). Due a larger network of capillary pores, the reference samples presented a higher absorption capacity (capillary suction) and greater difficulty in losing this moisture (lower porosity) than the other samples.

The tests were interrupted when the "unsafe potential" was reached in samples in the dry state. For a better view, these results are presented in Fig. 13. As can be seen, the reinforcing bars in specimens containing red mud took longer to depassivate than the reference samples, regardless of the amount of red mud added.

These results indicate only the onset of the corrosion process, without, however, presenting quantitative information about the phenomenon. Although they reached the end of test more quickly, the specimens that reached the unsafe potential continued to be subjected to wetting and drying cycles for up to 180 days, when the last samples (10%) reached this potential. Thus, it was possible to calculate the corrosion rate of all the samples according to Eq. (1). The results are shown in Fig. 14.

According to these results, the higher the content of red mud the lower the corrosion rate, which reached stability between 20 wt.% and 30 wt.% of red mud content. This behavior may be due to three isolated factors or to their combination: i) increasing alkalinity in the region near the steel-concrete interface; and/or ii) greater anchoring of chloride ions due to the presence of sodium aluminosilicates, which prevent the free movement of these ions and make them unavailable to start the corrosion process, as discussed with respect to the results of the chloride migration test; and/or iii) according to McCarter *apud* Santos [14], larger pores (existing in the specimens containing red mud) lose water more easily than the small and tortuous pores that are present in the reference sample.

Therefore, no clear correlation was found between rebar depassivation time and corrosion rate, i.e., the rebar corrosion process may begin sooner, but after this moment, the corrosion process may occur at a lower rate. However, this may have occurred simply due to our reliance on the parameters defined in the ASTM 876 standard to determine the onset of corrosion and the variation in the half-cell potential measured by our technique with the location of the anodic areas on the rebar surface.

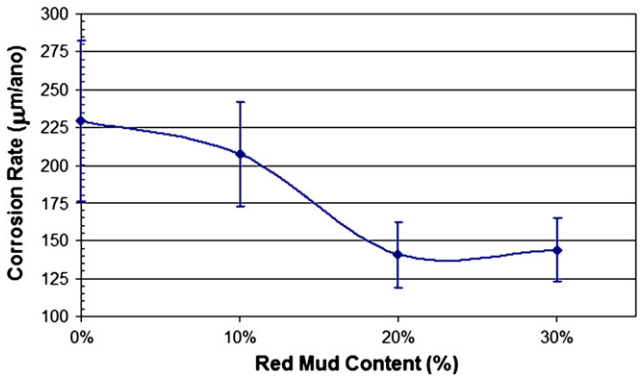

Fig. 14. Corrosion rate of steel bars embedded in reinforced concrete specimens, calculated after the corrosion potential test, as a function of red mud content.

The specialized literature offers controversial explanations about phenomena involving corrosion potentials. However, it seems there is a consensus that this technique is insufficient and should always be accompanied by some other technique to quantitatively determine the corrosion kinetics of rebars [24,25].

3.4. Electrical resistivity

Electrical resistivity is a property widely used to monitor concrete structures because it is a nondestructive method and allows for external monitoring by means of embedded electrodes. This property is fundamentally related to fluid permeability and to ion diffusivity through concrete pores.

Several authors [14,16,26–28] have shown that electrical resistivity is related to the microstructural characteristics of the cement matrix, such as porosity, pore size distribution, pore connectivity, and the conductivity of the aqueous solution in the matrix. In this study, three specimens were prepared for each amount of red mud content, providing a total of six results (each specimen yielded two different measures because of the two electrodes embedded at different measuring depths).

Fig. 15 shows the average results of the electrical resistivity of the reference specimens (0%) and the specimens containing red mud additions (10%, 20% and 30%). The specimens were kept in a moist chamber up to the age of 28 days, and the dotted lines in the figure represent the corrosion risk levels: high (<10 KΩ.cm), moderate (10–50 KΩ.cm), low (50–100 KΩ.cm), and insignificant (>100 KΩ.cm), according to the COST 509.

All the samples showed increased electrical resistivity due to increased paste hydration and to the reduction of fluid concentration in concrete pores as the specimens became increasingly dry, making them less conductive. According to Andrade [15] and Santos [14], the conduction of electrical current through concrete occurs through continuous pores and microcracks that are present in the matrix and filled with water.

The behavior of the specimens differed significantly according to different moisture contents. Among the specimens that were kept in the moist chamber (up to 28 days), the samples containing red mud were more resistive than the reference samples (0%). This effect continued to be visible in the first days after the specimens' removal from the moist chamber.

After drying the specimens, the reference samples showed a high increase in resistivity which exceeded that of the 40 to 80-day-old samples containing red mud. This effect can be explained by the high ionic concentration of red mud, which becomes more pronounced and active as the moisture content decreases when

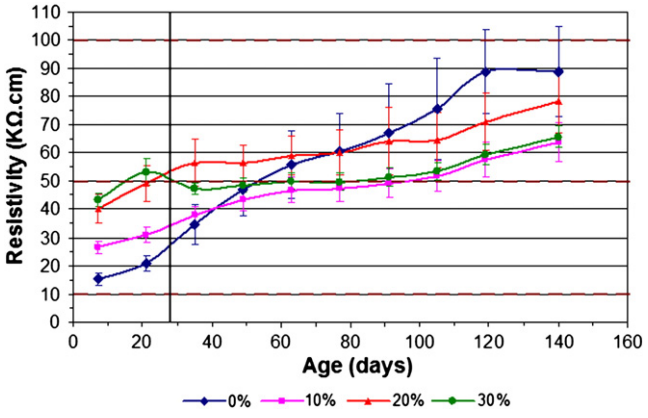

Fig. 15. Electrical resistivity of concrete specimens containing red mud, as a function of age.

Table 4
Equivalent conductivity of aqueous ions in infinite concentrations at 25 °C (Adamson *apud* Shi [24]).

Ion	Na^+	K^+	Ca^{2+}	SO_4^{2-}	OH^-	Cl^-
λ_0 ($m^{-1}\Omega^{-1}$)	0.00501	0.00735	0.00595	0.00798	0.0198	0.00763

compared to reference samples. A similar behavior was observed by Whiting and Nagi [26].

The equivalent electrical conductivities of aqueous ions typically found in concrete pores were determined by Adamson *apud* Shi [24] and these values are presented in Table 4. As can be seen, the Na^+, OH^-, Ca^{2+} and K^+ ions in red mud are highly conductive, contributing to lower the resistivity of concrete when it loses moisture.

Another factor to be considered is the higher porosity of concrete specimens containing red mud, which contributes decisively in reducing resistivity. Although they showed lower resistivity values than the reference samples, the samples of concrete containing red mud showed values well above the limit considered as low corrosion probability (>50 KΩ.cm). Hence, even if the presence of red mud does not prevent the occurrence of corrosion, it also cannot be considered harmful.

Another positive analysis factor is that the specimens containing red mud showed a higher resistivity in a humid environment, which is more conducive to corrosion. Unfortunately no measurements were taken of specimens kept moist throughout the experiment in order to verify if this behavior would be maintained.

3.5. Correlations

To assess the reliability of the results and determine if the addition of red mud gives reinforced concrete a stable behavior, several correlations are made between the results obtained by different techniques, as shown below.

3.5.1. Diffusion coefficients vs. corrosion potential

The correlation between the diffusion coefficients and corrosion rate obtained by the corrosion potential test is shown in Fig. 16.

This figure shows a directly proportional correlation between the diffusion coefficients and the corrosion rate, confirming that the higher penetration of chloride ions leads to a higher corrosion rate. The correlation coefficients were also quite satisfactory ($R^2 = 0.8460–0.9635$).

Thus, according to our analysis of the correlations between results obtained by different methods and involving different corrosion mechanisms, our conclusions about the performance of red mud as a concrete additive can be considered the most consistent, since they fully satisfy the scientifically accepted correlations.

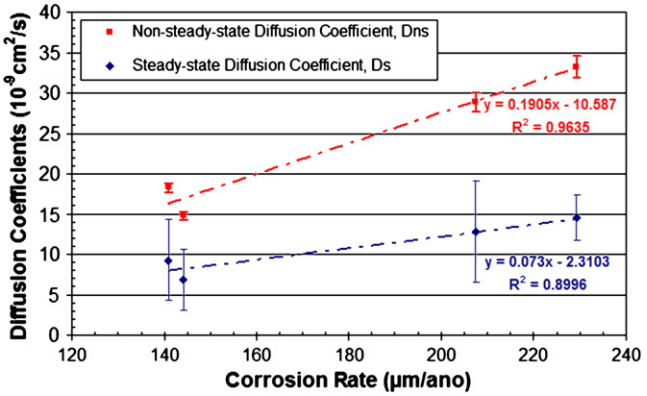

Fig. 16. Correlation between the diffusion coefficients and the corrosion rate obtained by the corrosion potential test.

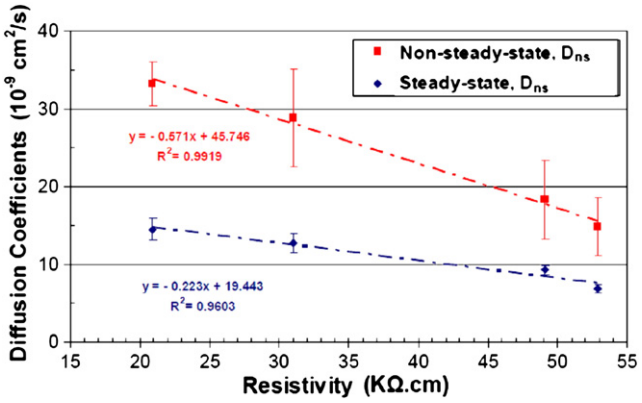

Fig. 17. Correlation between the diffusion coefficients and the electrical resistivity obtained by the corrosion potential test measured at 21 days of age in concrete specimens containing red mud and kept in a humid environment.

3.5.2. Diffusion coefficients vs. electrical resistivity

Recent researches [14,16,27] indicate that there is an inverse relationship between the resistivity and the chloride penetration of concrete. In this study, these variables could not be correlated because the conditions of measurement and maintenance of the specimens differed. While the resistivity test was conducted on nearly dry samples, the chloride migration tests were performed on moist samples. However, an analysis was made of the results obtained at 21 days (last resistivity measurement taken of the samples in the moist chamber). In this situation, an inversely proportional correlation was observed, as shown in Fig. 17.

Albeit inconclusive, this result is an indication that the correlation is valid for concrete samples containing red mud and kept in a humid environment, which is the most favorable situation for corrosion. Thus, the higher the concrete's resistivity, the lower the penetration of chloride ions and hence, the lower the probability of corrosion.

3.5.3. Corrosion potential vs. electrical resistivity

Fig. 18 shows the correlation between the resistivity results and the corrosion rate obtained by corrosion potential test. As expected, the correlation between resistivity and corrosion rate is inverse, confirming the principle that a higher resistivity is associated with a lower rate of corrosion. The correlation coefficients, R^2, are quite satisfactory (0.9466 and 0.9048).

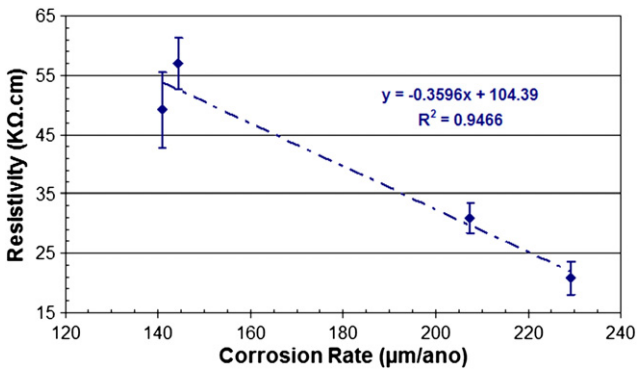

Fig. 18. Correlation between electrical resistivity and corrosion rate obtained by the corrosion potential test.

4. Conclusions

Based on an analysis of the results, the following conclusions can be drawn:

- The time lag increases with increasing red mud content as a result of the reduction in the relative amount of capillary pores.
- The decrease in the interconnectivity between capillary pores in samples containing red mud and the presence of typical mineralogical phases such as sodium aluminosilicates, known as sodalites, are responsible for reducing the flow of chloride ions, and hence, the steady-state and nonsteady-state diffusion coefficients.
- Electrical resistivity is a good indicator of the possible occurrence of chloride ion penetration. Thus, the higher the concrete's resistivity, the lower the penetration of chloride ions, and hence, the lower the probability of corrosion.
- The degree of saturation (humidity) of the concrete samples containing red mud appears to exert a considerable influence on the concrete's resistivity.
- The concrete specimens containing red mud presented higher resistivity in a humid environment, which is more favorable for corrosion.
- Evaluating the evolution of the corrosion process by corrosion potential tests is not possible; moreover, this technique only indicates the possibility of corrosion occurring, and should therefore be used as a complementary technique.
- The difference between the corrosion potential measures in wet and dry states is more pronounced in the reference samples (0%) which, due to their larger network of capillary pores, have a higher capacity to absorb solutions (capillary suction) and greater difficulty in losing this moisture (lower porosity) than samples containing red mud.
- The depassivation process of reinforcing bars is retarded by the presence of red mud.
- The higher the red mud content the lower the corrosion rate, which stabilizes between 20 wt.% and 30 wt.% of added red mud content.
- An inversely proportional correlation was observed between the resistivity and the chloride ion penetration in concrete containing red mud in samples subjected to the same saturation condition.
- The corrosion rate obtained by the corrosion potential test was inversely proportional to the electrical resistivity and directly proportional to the diffusion coefficients, and the results showed satisfactory correlation coefficients (R^2).

Acknowledgements

The authors wish to thank CNPq – National Council for Scientific and Technological Development (Brazil), PPGCEM/UFSCar – Postgraduate Program in Materials Science and Engineering at the Federal University of São Carlos (Brazil), and UA/DECV – Department of Ceramics and Glass Engineering, University of Aveiro & CICECO (Portugal) – Project FCT-PTDC/CTM/65243/2006.

References

[1] IBRAM – Brazilian Mining Association, BauxitaAvailable at, http://www.ibram.org.br/sites/1300/1382/00000033.pdf2009Access in october, 15th, 2010.
[2] ROSKILL REPORTS. The Economics of Bauxite & Alumina. Available at: <http://www.roskill.co.uk/index.html>. Access in june, 8th, 2010
[3] M. Singh, S.N. Upadhayay, P.M. Prasad, Preparation of special cements from red mud, Waste Manage. 16 (1996) 665–670.
[4] S.S. Amritphale, A. Anshula, N. Chandraa, N. Ramakrishnana, A novel process for making radiopaque materials using bauxite red mud, J. Eur. Ceram. Soc. 27 (2007) 1945–1951.
[5] S.S. Amritphale, M. Patel, Utilisation of red mud, fly ash for manufacturing bricks with pyrophyllite, Silicates Indus. 2 (1987) 31–35.
[6] J.N. Gordon, W.R. Pinnock, M.M. Moore, A preliminary investigation of strength development in Jamaican red mud composites, Cem. Concr. Compos. 18 (1996) 371–379.
[7] M.S. Vincenzo, C. Renz, M. Stefano, C. Giovanni, Bauxite red mud in the ceramic industry. Part 2: production of clay based ceramics, J. Eur. Ceram. Soc. 20 (2000) 245–252.
[8] N. Yalcin, V. Sevnic, Utilization of bauxite waste in ceramic glazes, Ceram. Int. 26 (2000) 485–493.
[9] P. Asokan, M. Saxean, S.R. Asolekar, Coal combustion residues-environmental implications and recycling potentials, Resour. Conserv. Recycl. 43 (2005) 239–262.
[10] P.E. Tsakirids, S. Agatzini-Leonardou, P. Oustadakis, Red mud addition in the raw meal for the production of Portland cement clinker, J. Hazard. Mater. B116 (2004) 103–110.
[11] M. Singh, S.N. Upadhayay, P.M. Prasad, Preparation of iron rich cements using red mud, Cem. Concr. Res. 27 (1997) 1037–1046.
[12] M. Castellote, C. Andrade, C. Alonso, Measurement of the steady and non-steady-state chloride diffusion coefficients in a migration test by means of monitoring the conductivity in the anolyte chamber. Comparison with natural diffusion tests, Cem. Concr. Res. 31 (2001) 1411–1420.
[13] L. Tong, O.E. Gjørv, Chloride diffusivity based on migration testing, Cem. Concr. Res. 31 (2001) 973–982.
[14] L. Santos. Evaluation of the Electrical Resistivity of Concrete as a Parameter to Calculation of the Initiation Period of Corrosion Induced by Chlorides in Concrete Structures. PhD thesis. Brasilia (Brazil), University of Brasilia (UNB), 2006, 161p.
[15] C. Andrade, Calculation of diffusion coefficients in concrete from ionic migration measurements, Cem. Concr. Res. 23 (1993) 724–742.
[16] R.B. Polder, Test methods for on site measurement of resistivity of concrete – a RILEM TC-154 technical recommendation, Constr. Build. Mater. 15 (2001) 125–131.
[17] E. Bauer. Comparative evaluation of the blast furnace slag addition influence in reinforcement corrosion by electrochemical techniques. PhD thesis. São Paulo (Brazil), University of São Paulo (USP), 1995, 236p.
[18] D.V. Ribeiro, J.A. Labrincha, M.R. Morelli, Use of red mud as addition for portland cement mortars, J. Mater. Sci. Eng. 4 (2010) 1–9.
[19] G. Song, Equivalent circuit model for SAC electrochemical impedance spectroscopy of concrete, Cem. Concr. Res. 30 (2000) 1723–1730.
[20] P.C. Aïtcin, The durability characteristics of high performance concrete: a review, Cem. Concr. Compos. 25 (2003) 409–420.
[21] D. Chvedov, S. Ostap, T. Le, Surface properties of red mud particles from potentiometric titration, Colloids Surf., A. 182 (2001) 131–141.
[22] E. Lopez, B. Soto, M. Arias, Adsorbent properties of red mud and its use for wastewater treatment, Water Res. 32 (1998) 1314–1322.
[23] V.S. Yadav, M. Prasad, J. Khan, S.S. Amritphale, M. Singh, C.B. Raju, Sequestration of carbon dioxide (CO_2) using red mud, J. Hazard. Mater. 176 (2010) 1044–1050.
[24] C. Shi, Effect of mixing proportions of concrete on its electrical conductivity and the rapid chloride permeability test (ASTM C1202 or ASSHTO T277) results, Cem. Concr. Res. 34 (2004) 537–545.
[25] J.M. Miranda, A. Cobo, E. Otero, J.A. González, Limitations and advantages of electrochemical chloride removal in corroded reinforced concrete structures, Cem. Concr. Res. 37 (2007) 596–603.
[26] D.A. Whiting, M.A. Nagi, Electrical Resistivity of Concrete — A Literature Review, Portland Cement Association, Illinois, USA, 2003, 57p. (R&D Serial No. 2457).
[27] P.A.M. Basheer, P.R.V. Gilleece, A.E. Long, W.J. Mc Carter, Monitoring electrical resistance of concretes containing alternative cementitious materials to assess their resistance to chloride penetration, Cem. Concr. Compos. 24 (2002) 437–449.
[28] W.J. McCarter, G. Starrs, T.M. Chrisp, Electrical conductivity, diffusion, and permeability of Portland cement-based mortars, Cem. Concr. Res. 30 (2000) 1395–1400.
[29] I. Odler, Special Portland cements, in: I. Odler (Ed.), Odler, Special inorganic cements, E and ;FN Spon Ed, 1999, pp. 7–45, London.
[30] J.M. Manso, J.A. Polanco, M. Losañez, J.J. González, Cem. Concr. Compos. 28 (2006) 528–534.
[31] C. Pellegrino, V. Gaddo, Cem. Concr. Compos. 31 (2009) 663–671.